Diagn Interv Radiol 2025; DOI: 10.4274/dir.2025.253513

ARTIFICIAL INTELLIGENCE AND INFORMATICS

ORIGINAL ARTICLE

Potential radiation dose reduction in computed tomography with deep learning reconstruction: a retrospective monocentric study

Lucas Graber[1]
Melike Zeynep Akış[2]
François Séverac[3]
Luc Mertz[4]
Serhat Akış[2]
Catherine Roy[1]
Mickaël Ohana[1]

[1]Hôpital Civil, Department of Radiology, Strasbourg, France

[2]Dokuz Eylül University Hospital, Department of Radiology, İzmir, Türkiye

[3]Université de Strasbourg, Department of Biostatistics and Informatics, Strasbourg, France

[4]Université de Strasbourg, Department of Radiation Safety and Radiophysics, Strasbourg, France

PURPOSE

To evaluate whether deep learning reconstruction (DLR) can reduce the radiation dose in routine clinical computed tomography (CT) scans compared with iterative reconstruction (IR) while maintaining or improving image quality. The study assesses DLR's consistency and effectiveness across four distinct CT protocols—chest, head, chest–abdomen–pelvis (CAP) oncology, and lower limb CT angiography (CTA)—representing a wide range of clinical applications.

METHODS

Our study is retrospective and monocentric. It involves a total population of 13,060 patients who underwent a CT scan using either a DLR algorithm (CT-DLR) or an IR algorithm (CT-IR) in one of four different CT acquisition protocols. Image quality was evaluated qualitatively and quantitatively by measuring standardized signal-to-noise ratio and contrast-to-noise ratio values. Assessment was performed on a subsample of 200 patients (25 per protocol per group).

RESULTS

The overall reduction in radiation dose for the CT-DLR group compared with the CT-IR group was approximately 20%. By protocol, dose reductions were 22% for chest CT, 21% for CAP oncology, 20% for lower limb CTA, and 19% for head CT. The CT-DLR group exhibited superior subjective and objective image quality to the CT-IR group.

CONCLUSION

DLR algorithms allow for a significant reduction in radiation dose while achieving higher image quality compared with IR algorithms.

CLINICAL SIGNIFICANCE

This large-scale study confirms that DLR can significantly reduce the radiation dose in routine CT imaging while maintaining or enhancing diagnostic image quality. Its consistent performance across multiple protocols supports broader clinical adoption. Notably, the greatest dose reductions were observed in high-use protocols such as chest and CAP CT, underscoring DLR's potential to improve both individual patient care and long-term population-level radiation safety.

KEYWORDS

Deep learning reconstruction, radiation dose reduction, computed tomography scan, image quality

Corresponding author: Melike Zeynep Akış

E-mail: melikemza7@gmail.com

Received 16 June 2025; revision requested 27 July 2025; last revision received 21 September 2025; accepted 24 October 2025.

Epub: 05.12.2025

DOI: 10.4274/dir.2025.253513

The exponential growth in computational power over the last two decades has enabled substantial improvements in computed tomography (CT) image reconstruction techniques.[1] Statistical-based iterative reconstruction (IR) and model-based IR techniques were introduced between 2000 and 2010,[2-4] resulting in a major reduction in image noise and the optimization of the signal-to-noise ratio (SNR) and the contrast-to-noise ratio (CNR) for lower irradiation doses,[5-8] yet with mixed results regarding pure image quality.

Recently, new image reconstruction methods have been developed using artificial intelligence-based techniques, such as deep learning with convolutional neural networks.[9] These neural networks are trained on tens of thousands of paired images to differentiate the noise

You may cite this article as: Graber L, Akış MZ, Séverac F, et al. Potential radiation dose reduction in computed tomography with deep learning reconstruction: a retrospective monocentric study. *Diagn Interv Radiol.* December 2025 DOI: 10.4274/dir.2025.253513 [Epub Ahead of Print].

from the signal more efficiently, resulting in further improvements in image quality[10-13] as well as a reduction in the radiation dose delivered.[14-17]

Although many studies have highlighted the superiority of deep learning reconstruction (DLR) algorithms in terms of image quality compared with previous algorithms, their potential for radiation dose reduction has also been confirmed. Kobayashi et al.[18] demonstrated that the implementation of DLR reduced the radiation dose by 45% and lowered the estimated risk of radiation-induced cancer from 0.247% to 0.130%. Although their modeling approach illustrates the theoretical potential of DLR, our study focuses on real-world clinical protocols, revealing a more moderate reduction of 20%. This contrast underscores the complementary value of both perspectives and motivates the present study by addressing routine practice applicability.

The main objective of our study is to estimate the potential radiation dose reduction that can be achieved in a real-life setting using a DLR algorithm compared with an IR algorithm while maintaining equivalent image quality. Our secondary objective is to investigate the variation in radiation dose reduction potential as a function of body mass index (BMI) and patient sex.

Methods

Ethics

Our study was a retrospective analysis of prospectively collected clinical data. The study design was approved by the Ethics Committee of Strasbourg University Hospital (decision number: RNI-2021-149, date: 14.12.2021), and written consent from participating patients was not required.

Main points

- Deep learning reconstruction (DLR) significantly reduces the radiation dose in routine computed tomography (CT) scans compared with iterative reconstruction, with an average reduction of 20%.
- Despite lower radiation, DLR provides consistently better or equivalent image quality across all evaluated protocols: chest CT, head CT, chest–abdomen–pelvis oncology, and lower limb CT angiography.
- These findings support the clinical implementation of DLR as a safe and effective reconstruction method for dose optimization in a wide range of CT applications.

Population

This is a retrospective, single-center study analyzing prospectively collected dosimetry data from the Dose Archiving and Communication System (DACS) of the diagnostic radiology department of the Nouvel Hôpital Civil (Strasbourg University Hospital) between May 2018 and May 2021. All patients who underwent CT examinations during this period and had their radiation dose data stored on the DACS were considered for inclusion.

Specifically, we included patients who underwent CT examinations on either a third-generation wide-area detector CT scanner equipped with IR software [Aquilion One Genesis, Canon Medical Systems, Ōtawara, Tochigi, Japan, with three-dimensional adaptive iterative dose reduction (AIDR-3D)], which served as the control group (CT-IR), or a fourth-generation wide-area detector CT scanner equipped with DLR [Aquilion One Prism, Canon Medical Systems, with the *Advanced intelligent Clear-IQ Engine* (AiCE)], which served as the test group (CT-DLR). The Genesis system is equipped with PUREViSION detectors, the AIDR-3D hybrid IR algorithm, and SUREExposure 3D dose modulation, providing 16-cm z-axis coverage suitable for whole-organ imaging. The Prism system, although offering the same 16-cm z-axis coverage, incorporates improved PUREViSION Optics with lower electronic noise and higher light-collection efficiency, enhanced dose-modulation features (including adaptive collimation and advanced exposure control), faster gantry rotation (up to 0.25 seconds), and optional single energy metal artifact reduction, in addition to the AiCE DLR algorithm. These hardware and software differences may have contributed to the observed reduction in radiation dose, in addition to the reconstruction algorithm itself.

Examinations had to meet predefined criteria, including being either a non-contrast chest CT, non-contrast head CT, chest–abdomen–pelvis (CAP) CT with injection, or CT angiography (CTA) of the lower limbs. Only examinations with a single series were included; thus, multiphasic CT was excluded.

A total of 13,060 patients were included in our study, with 4,361 patients in the CT-DLR group and 8,799 patients in the CT-IR group. Within the CT-DLR group, 1,567 patients were examined according to the chest CT protocol, 1,623 according to the head CT protocol, 1,109 according to the CAP oncology protocol, and 62 according to the lower limb CTA protocol. Within the CT-IR group, 3,060 patients were examined according to the chest CT protocol, 3,436 according to the head CT protocol, 2,058 according to the CAP oncology protocol, and 245 according to the lower limb CTA protocol (Figure 1).

To improve transparency and assess potential baseline imbalances between groups, we compiled a summary table of demo-

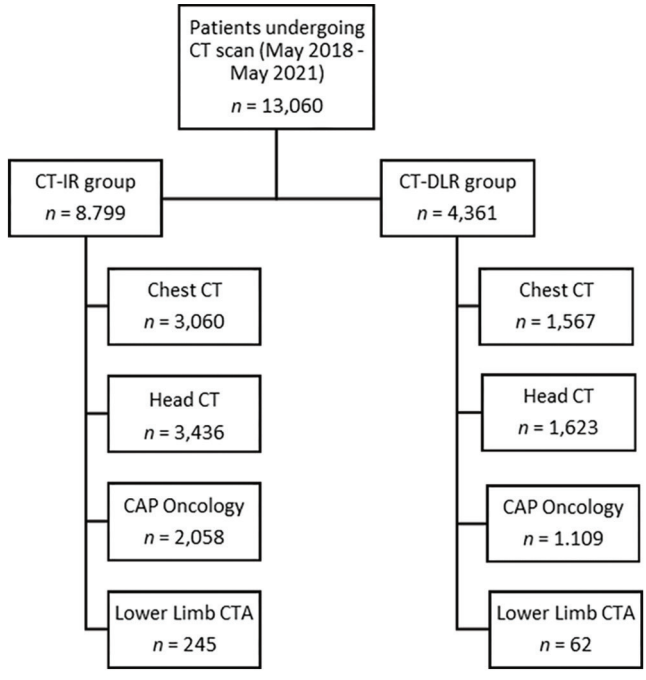

Figure 1. Flowchart of patient enrollment. CT-IR, computed tomography with iterative reconstruction; CT-DLR, computed tomography with deep learning reconstruction; CAP, chest–abdomen–pelvis; CTA, computed tomography angiography.

graphic characteristics, including age, sex distribution, BMI, and weight, for each protocol and reconstruction method (CT-IR and CT-DLR). These variables are known to affect radiation dose and were therefore reported to support comparability across groups (Table 1).

To homogenize data, examinations were selected based on anatomical area, contrast medium injection, and z-axis coverage (Table 2). The acquisition protocols were kept identical on both devices, except for the reconstruction algorithm used and the automatic z-axis dose modulation, which was adapted to these algorithms based on vendor recommendations.

Database

For each patient, we collected the date of the examination; the machine on which the examination was performed; the examination protocol; the patient's sex, weight, height, and BMI (if available); the dose–length product (DLP; mGy.cm); the CT dose index (mGy); the exposure time (ms); the acquisition field length (mm); the tube voltage (kV); and the tension (mA). The radiation protection team of Strasbourg University Hospital conducted the data extraction.

Image quality assessment

For the specific qualitative and quantitative image analysis, we randomly selected 25 patients from the CT-IR group for each of the four examination protocols, using a stratified random sampling method with probabilities proportional to height. The stratification variable was BMI, which was categorized into four classes (BMI <20, 20< BMI <25, 25< BMI <30, BMI >30) to approximate clinical thresholds for underweight, normal weight, overweight, and obesity, in line with World Health Organization guidelines.[19] These categories were chosen because patient body habitus substantially affects image noise and radiation dose modulation in CT examinations. This approach ensured that the sampled BMI distribution closely mirrored that of the overall study population.

Next, we selected 25 patients from the CT-DLR group using a 1:1 individual matching method that combined exact matching for sex and the nearest neighbor method for BMI. A caliper of $\pm$ 0.5 kg/m^2 was applied during BMI matching to ensure comparable body habitus between CT-DLR and CT-IR groups.

A sample size of 25 patients per protocol and per group (CT-DLR and CT-IR) was deemed sufficient for the paired comparison of image quality metrics based on SNR, CNR, and Likert scores. This sample size represents a practical balance between statistical robustness and the feasibility of manual image evaluation.

Qualitative analysis

We conducted a subjective analysis of image quality using a Likert scale ranging from 1 to 5, following the European guidelines on image quality.[20] The analysis was performed by a single radiologist (LG, with 4 years of experience in CT). Evaluation criteria included visibility of relevant anatomical structures, sharpness of tissue boundaries, perceived image noise, soft tissue contrast resolution, and presence of reconstruction-related artifacts. The Likert scale categories were as follows:

Table 1. Baseline characteristics of patients in each protocol group, stratified by reconstruction method (IR vs. DLR)

	Protocol	Group	Age (mean)	Sex (male/female)	Body mass index (mean)	Weight (mean)
1.	Head CT	IR	76	17 M/8 F	26.73	81
2.	Head CT	DLR	72	17 M/8 F	26.64	81
3.	Chest CT	IR	51	17 M/8 F	25.97	77
4.	Chest CT	DLR	57	17 M/8 F	25.98	77
5.	CAP oncology	IR	61	13 M/12 F	27.89	83
6.	CAP oncology	DLR	62	13 M/12 F	27.17	81
7.	Lower limb CTA	IR	64	19 M/6 F	24.92	74
8.	Lower limb CTA	DLR	68	19 M/6 F	25.35	75

IR, iterative reconstruction; DLR, deep learning reconstruction; M, male; F, female; CT, computed tomography; CTA, CT angiography.

Table 2. Acquisition protocols according to the type of examination (identical on both devices)

Protocol	Chest CT	Head CT	CAP oncology	Lower limb CTA
Helical volume acquisition number	Single	Single	Single	Single
PoC injection prior to acquisition	No	No	70 seconds	30 seconds
Anatomical zone	Thorax	Skull	Chest–abdomen–pelvis	Abdomen and lower limbs
Minimum and maximum coverage (cm)	20–60	9–40	50–100	100–180
Collimation	0.5 × 80	0.5 × 40	0.5 × 80	0.5 × 40
Kilovoltage (kV)	Automatically defined according to scout	120	Automatically defined according to scout	100
Milliampere (mA)	Modulation	Modulation	Modulation	Modulation
Rotation time (s)	0.275	0.75	0.5	0.4
Cutting thickness (mm)	1 every 0.8	1 every 0.8	1 every 0.8	1 every 0.8

PoC, point of contrast; CAP, chest–abdomen–pelvis; CTA, computed tomography angiography; CT, computed tomography.

1) non-diagnostic, 2) poor image quality, 3) limited image quality but diagnostic, 4) good image quality, and 5) optimal image quality.

Quantitative analysis

To ensure reproducibility and minimize inter-subject variability, all quantitative measurements (SNR and CNR) were standardized by using anatomically predefined, fixed-size regions of interest (ROIs). Background noise was consistently defined as the standard deviation of Hounsfield units within a homogeneous air region around the outside of the patient's body. This approach, adapted from prior validated methods, was based on Bhosale[21] and Chatzaraki et al.[22] for CAP oncology and lower limb CTA, Tang et al.[23] for chest CT, and Guziński et al.[24] for head CT.

Chest–abdomen–pelvis oncology and lower limb computed tomography angiography

Based on Bhosale,[21] we placed an axial slice ROI of approximately 20 mm² in the right liver parenchyma behind the vena cava (Figure 2), with another ROI of approximately 20 mm² in the abdominal subcutaneous fat when possible (the size of the ROI was reduced if the thickness of the adipose tissue was insufficient) to measure the mean value. In cases where the adipose tissue thickness was insufficient, the size of the ROI was reduced accordingly. Although smaller ROIs are known to be more susceptible to local noise, potentially influencing the reproducibility of the SNR and CNR measurements—particularly in low-contrast regions—ROIs were carefully placed in homogeneous areas to mitigate this effect. This approach is consistent with the methodological considerations discussed in prior studies, including Chatzaraki et al.[22] A similarly sized ROI was placed in the background around the outside of the patient to measure the distribution (standard deviation) of voxel values.

According to the literature review by Chatzaraki et al.,[22] the most reliable and reproducible method for calculating the SNR and CNR in images is to use the distribution of voxel values in the background as the denominator.

The SNR is calculated as follows:

$$\frac{Vmean(liver)}{\sigma(background\ noise)}$$

The CNR is calculated as follows:

$$\frac{Vmean(liver)-Vmean(fat)}{\sigma(background\ noise)}$$

Chest computed tomography

We measured the mean voxel value by placing an ROI in the descending thoracic aorta, covering approximately half of the aortic lumen area in the axial section (Figure 2), similar to the study by Tang et al.[23] We also measured the mean voxel value in the adipose tissue of the left axillary region, using an ROI of at least 50 mm², and we placed an ROI of at least 50 mm² in the background around the outside of the patient to measure the voxel value distribution (standard deviation).

The SNR is calculated as follows:

$$\frac{Vmean(Aorta)}{\sigma(background\ noise)}$$

The CNR is calculated as follows:

$$\frac{Vmean(Aorta)-Vmean(fat)}{\sigma(background\ noise)}$$

Head computed tomography

We followed a method similar to that of Guziński et al.[24] We measured the mean voxel value in an ROI of at least 20 mm² located in the anterior portion of the right caudate nucleus in the axial slice (Figure 2). We also measured the mean voxel value in a similarly sized ROI of the fourth ventricle and an ROI with a minimum area of 10 mm² in the background around the outside of the patient to measure the distribution (standard deviation) of the voxel value.

The SNR is calculated as follows:

$$\frac{Vmean(Basal\ ganglia)}{\sigma(background\ noise)}$$

The CNR is calculated as follows:

$$\frac{Vmean(Basal\ ganglia)-Vmean(CSF)}{\sigma(background\ noise)}$$

The position of these ROIs was optimized to minimize the variation in voxel values within them.

Statistical analysis

General population

Continuous variables are reported as mean ± standard deviation, whereas categorical variables are presented as counts and proportions. To analyze the radiation exposure, linear regression models were used. Extreme values of radiation exposure (> 95th percentile) were excluded from the models, as they may be caused by technical issues or multiple acquisitions during the same examination (such as patient movements and injection problems); their exclusion was intended to reduce the undue influence of outliers and improve the robustness of the analysis by focusing on typical cases.

To evaluate the independent effects of different factors, a multivariate model, including scanner type, protocol type, BMI, and sex, was constructed. Pairwise interactions between scanner type and other factors of interest were also included in the model to determine whether the effect of scanner type was dependent on other factors. The normality of the residuals was assessed using a quantile–quantile plot. The results are presented as differences with 95% confidence intervals (CIs).

Random samples

The analyses of image quality, SNR, and CNR were conducted on randomly selected samples with individual matching. Therefore, comparisons of the different variables of interest between the two types of scanners were performed using paired tests. Continuous variables were compared using the Wilcoxon signed-rank test, and categorical variables were compared using the Stuart–Maxwell test. A P value < 0.05 was considered statistically significant. The analyses were performed using R software version 4.1.1. (R Core Team, Vienna, Austria).

Results

Population

A total of 13,060 patients were included in the study—4,361 in the CT-DLR group and 8,799 in the CT-IR group—covering a range of clinical protocols: chest CT, head CT, CAP oncology, and lower limb CTA. Baseline demographic characteristics for each protocol and reconstruction group are summarized in Table 1.

Overall results

Compared with the CT-IR group, overall irradiation was significantly lower in the CT-DLR group, with a difference of 86.6 DLP units (95% CI: 78.5, 94.6; P < 0.001), corresponding to a radiation dose reduction of approximately 20%.

Further analysis by protocol showed an average reduction of 19.3% (95% CI: -21.6, -17) for head CT, 21.8% (95% CI: -24.1, -18.3) for chest CT, 20.9% (95% CI: -26.8, -20.2) for CAP

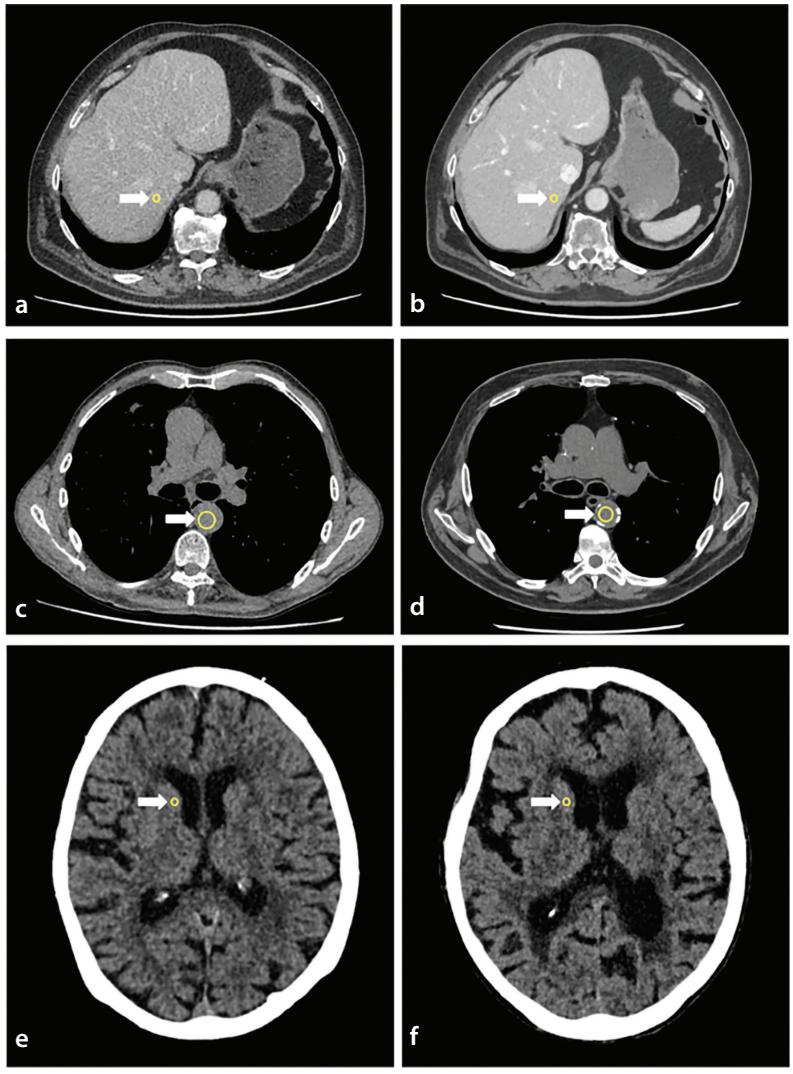

Figure 2. Representative axial computed tomography (CT) images from different anatomical regions and reconstruction algorithms: **(a)** and **(b)**. Abdominal CT images from two different patients, reconstructed with iterative reconstruction (IR) and deep learning reconstruction (DLR), respectively. In both, a white arrow indicates a region of interest (ROI) placed in the right liver parenchyma posterior to the inferior vena cava: **(c)** and **(d)**. Chest CT images reconstructed with IR and DLR, respectively. In both images, a white arrow indicates an ROI placed in the descending thoracic aorta in the axial section: **(e)** and **(f)**. Head CT images from two different patients, reconstructed with IR and DLR, respectively. In both, a white arrow indicates an ROI placed in the anterior portion of the right caudate nucleus for mean voxel value measurement.

oncology, and 19.5% (95% CI: -30.4, -7.0) for lower limb CTA in the CT-DLR group (Figure 3).

Multivariate analysis adjusting for BMI showed that male patients had a mean excess radiation of 47.9 DLP units ($P < 0.001$), corresponding to a 12% difference in delivered radiation dose. However, there was no significant difference between the CT-DLR and CT-IR groups [47.8 (95% CI: 41.6, 54.1) vs. 47.9 (95% CI: 43.2, 52.7), $P = 0.965$], indicating that the dose reduction achieved with DLR was consistent across sexes.

In terms of BMI, there was no significant difference in irradiation between the two groups for the head CT and lower limb CTA protocols. However, for the chest CT protocol, patients with BMI >30 showed a significant increase in dose reduction with DLR compared with those with BMI <20 [-62.1 (95% CI: -73.8, -49.1) vs. -30.7 (95% CI: -46.6, -14.9), $P = 0.003$]. Similarly, for the CAP oncology protocol, patients with BMI between 25 and 30 and those with BMI >30 showed a significant increase in dose reduction in the CT-DLR group compared with the CT-IR group [-115.8 (95% CI: -129.5, -102.1) and -131.0 (95% CI: -150.7, -111.4) vs. -57.6 (95% CI: -80.4, -34.9), $P < 0.001$ for both comparisons] (Figure 4).

Results samples

Table 3 displays the mean values for the SNR, CNR, and Likert scores used to assess image quality. Regardless of the acquisition protocol, the CT-DLR group exhibited significantly higher SNR, CNR, and Likert score values than the CT-IR group ($P < 0.001$).

Figure 5 displays the distribution of CNR values using a box-and-whisker plot.

Discussion

In a real-life retrospective analysis of over 10,000 CT examinations, we demonstrated that the use of DLR leads to a meaningful reduction in radiation dose compared with IR, with an average decrease of approximately 20%. This reduction was consistent and statistically significant across all four protocols, being most notable in the chest CT protocol and least notable in the head CT protocol. The observed differences remained significant even after adjusting for patient characteristics such as BMI and sex. Notably, dose reduction was greater in patients with higher BMI, especially in the CAP oncology

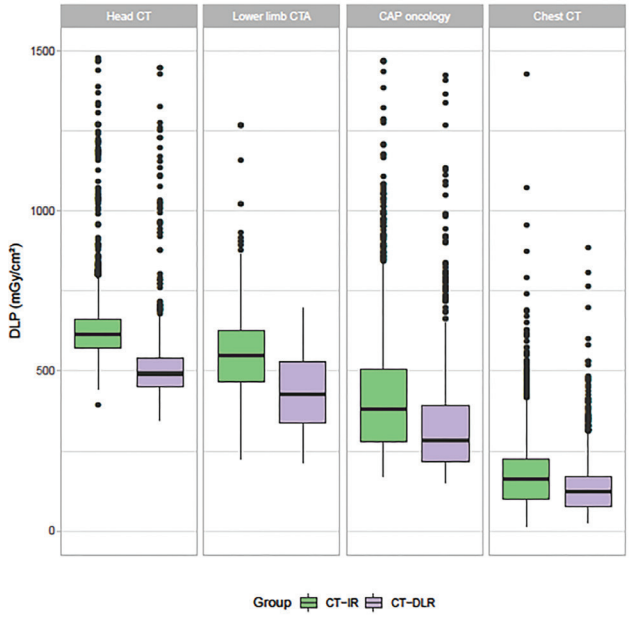

Figure 3. Box-and-whisker plot showing the distribution of patient dose by scanner type and acquisition protocol. DLP, dose–length product; CT-IR, computed tomography with iterative reconstruction; CT-DLR, computed tomography with deep learning reconstruction; CAP, chest–abdomen–pelvis; CTA, computed tomography angiography.

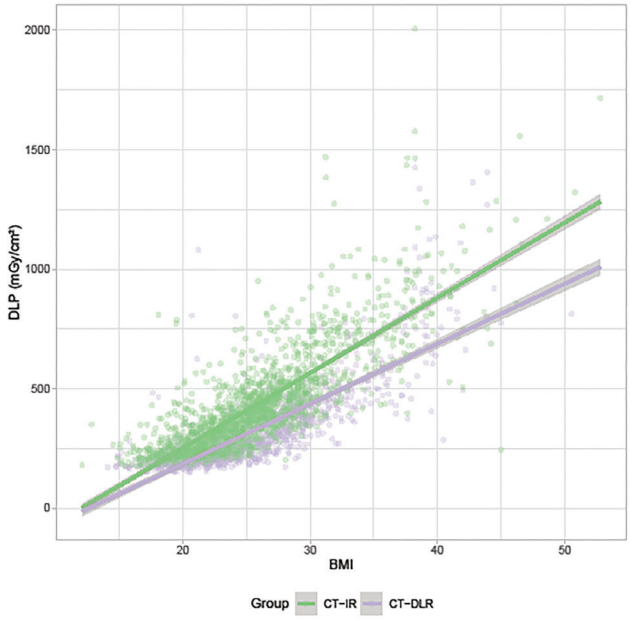

Figure 4. Correlation curves showing the radiation dose delivered to patients in relation to their body mass index. DLP, dose–length product; CT-IR, computed tomography with iterative reconstruction; CT-DLR, computed tomography with deep learning reconstruction; BMI, body mass index.

and chest CT protocols. Image quality was qualitatively and quantitatively evaluated as being at least equivalent to that of IR, confirming the results already published in the literature,[16,17] while involving a larger number of patients.

The benefit of the DLR algorithm in terms of dose reduction compared with the IR algorithm appears to be slightly greater for the chest CT protocol than for the other protocols. This may be attributed to the lower attenuation of thoracic structures and the lung parenchyma having greater intrinsic contrast, making it more adapted to dose reduction.

Despite the dose reduction, we observed a superior objective (SNR, CNR) and subjective (Likert scale) image quality for each protocol, consistent with studies published in the literature.[11-13] The DLR algorithm seems to have a greater advantage in terms of image quality for the chest CT and CAP oncology protocols than for the head CT and lower limb CTA protocols. This could be explained by the predominance of soft tissue on the thorax and abdomen, which the DLR algorithm is more effective at handling, compared with the lower limbs and skull, which have a larger proportion of bony structures. For lower limb CTA, however, the limited number of DLR cases resulted in wide CIs, and these findings should therefore be regarded as exploratory.

The clinical implications of this dose reduction are considerable. A recent large-scale risk-projection study by Smith-Bindman et al.[25] estimated that approximately 103,000 future cancers may result from the 93 million CT examinations performed in the United States in 2023 alone. Notably, the largest share of projected cancers was attributed to CAP and chest CT scans—protocols in which we observed the highest dose reductions using DLR.[25] Hence, a consistent 20% reduction in radiation dose across these high-utilization protocols could potentially contribute to reducing radiation-induced cancer risk at the population level. These

Table 3. Average values of signal-to-noise ratio, contrast-to-noise ratio, and 5-point Likert score of image quality evaluated on the samples of the four protocols, according to the type of scanner

Protocol	Signal-to-noise ratio		Contrast-to-noise ratio		Image quality (Likert / 5)		*P* value*
	CT-DLR group	CT-IR group	CT-DLR group	CT-IR group	CT-DLR group	CT-IR group	
Chest CT	3.78	2.27	22.4	8.6	4.74	4	< 0.001
Lower limb CTA	61.49	46.24	78.74	58.24	4.8	4.32	< 0.001
CAP oncology	18.71	7.32	35.33	13.84	4.96	4.52	< 0.001
Head CT	13.7	13.3	13.6	12.6	4.36	3.88	< 0.001

*Wilcoxon signed-rank test (continuous variables) and Stuart–Maxwell test (categorical variables). CT-DLR, computed tomography with deep learning reconstruction; CT-IR, computed tomography with iterative reconstruction; CTA, computed tomography angiography; CAP, chest–abdomen–pelvis.

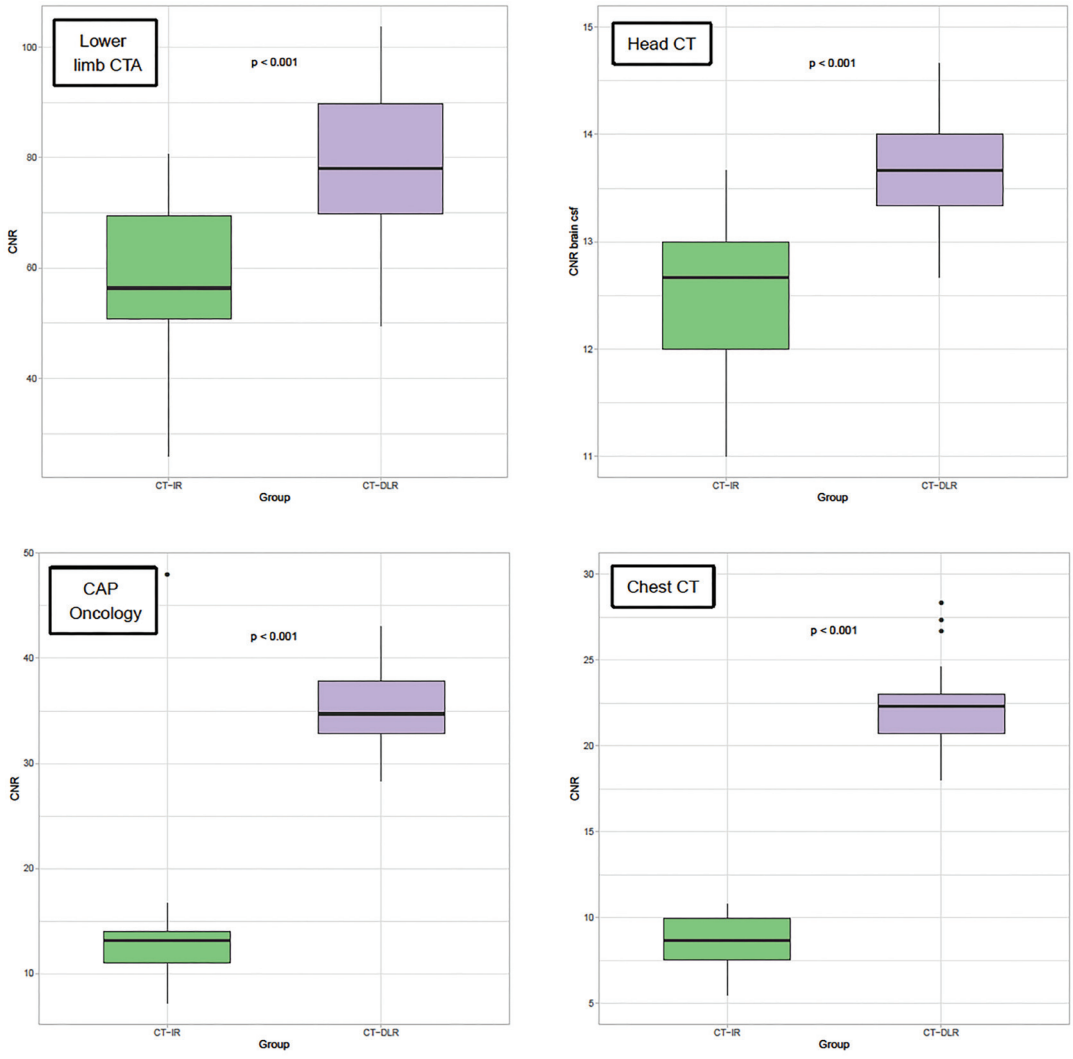

Figure 5. Box-and-whisker plot showing the distribution of the contrast-to-noise ratio for each scanner type and protocol. CTA, computed tomography angiography; CAP, chest–abdomen–pelvis.

findings highlight the dual benefit of DLR: achieving superior image quality while also supporting long-term cancer risk mitigation. A recent study by Kobayashi et al.[18] demonstrated that the implementation of DLR could reduce the radiation dose by up to 45% and, importantly, lower the projected risk of radiation-induced cancer compared with IR. Taken together with our finding of a consistent 20% dose reduction in a large real-life cohort, these results underscore the broader clinical importance of adopting DLR, highlighting its potential not only for routine dose optimization but also for contributing to long-term patient safety.

Additionally, we found that male patients received, on average, 48 DLP units (approximately 12%) more radiation than female patients, independent of the type of examination, scanner, or BMI. This finding indicates a potential sex-related difference in radiation dose. However, the current literature on this topic is limited, and further dedicated investigations are required to better understand the underlying factors and confirm this observation.

We were able to demonstrate that the difference in irradiation between the two scanners is significantly greater for higher BMIs in the CAP oncology and lower limb CTA protocols. This difference may be attributed to the DLR algorithm's superior ability to eliminate artifacts associated with anatomical factors related to body structure, thereby maintaining satisfactory image quality with more effective dose modulation.

Another important aspect to consider is that the CT-IR and CT-DLR groups were scanned on different generations of scanners (Aquilion One Genesis vs. Aquilion One Prism). Although acquisition protocols were identical, the fourth-generation Prism integrates incremental hardware advances such as improved detector efficiency, lower electronic noise, and more sophisticated dose modulation. Consequently, the 20% reduction in radiation dose observed in our study should not be attributed solely to the DLR algorithm but rather to the combined contribution of both reconstruction and hardware improvements. This potential confounding effect is important when interpreting our results and may partly explain the variability in dose reduction observed across protocols and patient subgroups.

Our findings of an average 20% reduction in radiation dose with DLR differ from the 45% reduction reported by Kobayashi et al.,[18] who additionally performed lifetime attributable risk modeling. Several factors may explain this discrepancy. First, scanner hardware generation differed: our analysis compared the Aquilion One Genesis (IR) with the newer Aquilion One Prism (DLR), whereas Kobayashi et al.[18] employed the Aquilion Precision. Such differences in de-

tector design, dose modulation, and overall system architecture may partly confound the isolated contribution of the reconstruction algorithm. Second, protocol composition differed: our study included a broader range of routine protocols (head CT, chest CT, CAP oncology, and lower limb CTA), whereas Kobayashi et al.[18] focused solely on body CT examinations (e.g., abdomen and pelvis), potentially delivering a different dose distribution. Finally, methodological differences must be acknowledged, particularly their use of risk-projection modeling vs. our emphasis on real-world clinical applicability. Taken together, these differences suggest that although absolute dose-reduction magnitudes may vary depending on study design, scanner generation, and protocol composition, the available evidence—including our large real-world cohort—supports the potential of DLR to meaningfully reduce patient radiation exposure.

Our study has several limitations that should be acknowledged. First, due to its retrospective design, it was not possible to strictly match patients between the CT-IR and CT-DLR groups. Additionally, the number of patients scanned with IR was higher, as the IR-equipped scanner was installed earlier and thus had a longer period of data collection. This temporal difference may have introduced slight variations in patient characteristics, possibly influenced by individual radiologists' preferences for one scanner over the other. Nonetheless, no statistically significant differences were observed between the two populations. As a further limitation, being a single-center non-randomized study, some degree of temporal or operator-related bias cannot be entirely excluded, particularly given the longer accrual period of the IR scanner.

Being a single-center study, the generalizability of our results to other institutions or populations may be limited despite the large sample size. Some inaccuracies in protocol labeling may also have occurred, such as injected head CTs being mislabeled or CAP oncology scans being performed without contrast. These errors did not affect the radiation dose measurements and only minimally influenced the SNR and CNR results in subgroup analyses.

A few extreme values were excluded during multivariate modeling to ensure robust analysis; however, the exclusion rate was balanced across both groups. In addition, qualitative and quantitative image assessments were performed by a single radiologist with 4 years of CT experience. Although full blinding was not feasible due to the visually distinguishable differences between IR and DLR images, the consistency between subjective Likert scores and objective metrics (SNR, CNR), together with concordance with the existing literature, supports the validity of our findings. Furthermore, the small sample size in the lower limb CTA subgroup limits the precision of dose estimates, and these results should be interpreted with caution.

Finally, because IR and DLR data were acquired on scanners from different generations, hardware advances in the Prism system may have contributed to the observed dose reduction, representing a potential confounding factor.

In conclusion, in this retrospective study, we found that implementing DLR algorithms resulted in a mean 20% reduction in radiation dose compared with IR algorithms, across a wide range of patients and scanning protocols, with—at least—non-inferior qualitative and quantitative image quality. Future studies could explore the difference in radiation dose between men and women, independent of other factors, and determine the optimal balance between dose reduction and image quality enhancement offered by these DLR algorithms.

Acknowledgements

The authors would like to thank the Department of Radiology at both Hôpital Civil, Strasbourg and Dokuz Eylül University Hospital for their valuable support.

Footnotes

Conflict of interest disclosure

The authors declared no conflicts of interest.

References

1. Willemink MJ, Noël PB. The evolution of image reconstruction for CT-from filtered back projection to artificial intelligence. *Eur Radiol*. 2019;29(5):2185-2195. [Crossref]
2. Patino M, Fuentes JM, Singh S, Hahn PF, Sahani DV. Iterative reconstruction techniques in abdominopelvic CT: technical concepts and clinical implementation. *AJR Am J Roentgenol*. 2015;205(1):W19-31. [Crossref]
3. Southard RN, Bardo DME, Temkit MH, Thorkelson MA, Augustyn RA, Martinot CA. Comparison of iterative model reconstruction versus filtered back-projection in pediatric emergency head CT: dose, image quality, and image-reconstruction times. *AJNR Am J Neuroradiol*. 2019;40(5):866-871. [Crossref]
4. Shuman WP, Green DE, Busey JM, et al. Model-based iterative reconstruction versus adaptive statistical iterative reconstruction and filtered back projection in liver 64-MDCT: focal lesion detection, lesion conspicuity, and image noise. *AJR Am J Roentgenol*. 2013;200(5):1071-1076. [Crossref]
5. Frija G. Recent updates in radioprotection. *Eur Radiol*. 2021;31(2):599-600. [Crossref]
6. Brady SL, Trout AT, Somasundaram E, Anton CG, Li Y, Dillman JR. Improving image quality and reducing radiation dose for pediatric CT by using deep learning reconstruction. *Radiology*. 2021;298(1):180-188. [Crossref]
7. Smith EA, Dillman JR, Goodsitt MM, Christodoulou EG, Keshavarzi N, Strouse PJ. Model-based iterative reconstruction: effect on patient radiation dose and image quality in pediatric body CT. *Radiology*. 2014;270(2):526-534. [Crossref]
8. Andersen HK, Völgyes D, Martinsen ACT. Image quality with iterative reconstruction techniques in CT of the lungs-a phantom study. *Eur J Radiol Open*. 2018;5:35-40. [Crossref]
9. Currie G, Hawk KE, Rohren E, Vial A, Klein R. Machine learning and deep learning in medical imaging: intelligent imaging. *J Med Imaging Radiat Sci*. 2019;50(4):477-487. [Crossref]
10. Akagi M, Nakamura Y, Higaki T, et al. Deep learning reconstruction improves image quality of abdominal ultra-high-resolution CT. *Eur Radiol*. 2019;29(11):6163-6171. Erratum in: *Eur Radiol*. 2019;29(8):4526-4527. [Crossref]
11. Shirasaka T, Kojima T, Funama Y, et al. Image quality improvement with deep learning-based reconstruction on abdominal ultrahigh-resolution CT: a phantom study. *J Appl Clin Med Phys*. 2021;22(7):286-296. [Crossref]
12. Singh R, Digumarthy SR, Muse VV, et al. Image quality and lesion detection on deep learning reconstruction and iterative reconstruction of submillisievert chest and abdominal CT. *AJR Am J Roentgenol*. 2020;214(3):566-573. [Crossref]
13. Liu P, Wang M, Wang Y, et al. Impact of deep learning-based optimization algorithm on image quality of low-dose coronary CT angiography with noise reduction: a prospective study. *Acad Radiol*. 2020;27(9):1241-1248. [Crossref]
14. Greffier J, Hamard A, Pereira F, et al. Image quality and dose reduction opportunity of deep learning image reconstruction algorithm for CT: a phantom study. *Eur Radiol*. 2020;30(7):3951-3959. [Crossref]
15. Nagayama Y, Goto M, Sakabe D, et al. Radiation dose optimization potential of deep learning-based reconstruction for multiphase hepatic CT: a clinical and phantom study. *Eur J Radiol*. 2022;151:110280. [Crossref]
16. Nam JG, Hong JH, Kim DS, Oh J, Goo JM. Deep learning reconstruction for contrast-enhanced

CT of the upper abdomen: similar image quality with lower radiation dose in direct comparison with iterative reconstruction. *Eur Radiol*. 2021;31(8):5533-5543. [Crossref]

17. Benz DC, Ersözlü S, Mojon FLA, et al. Radiation dose reduction with deep-learning image reconstruction for coronary computed tomography angiography. *Eur Radiol*. 2022;32(4):2620-2628. [Crossref]
18. Kobayashi N, Nakaura T, Yoshida N, et al. Impact of deep learning reconstruction on radiation dose reduction and cancer risk in CT examinations: a real-world clinical analysis. *Eur Radiol*. 2025;35(6):3499-3507. [Crossref]
19. Obesity: preventing and managing the global epidemic. Report of a WHO consultation. *World Health Organ Tech Rep Ser*. 2000;894:i-xii, 1-253. [Crossref]
20. European Commission. European guidelines on quality criteria for computed tomography [Internet]. Luxembourg: Publications Office of the European Union; 2000 [cited 2025 Nov 5]. [Crossref]
21. Bhosale P. Comparing CNR, SNR, and image quality of CT images reconstructed with soft kernel, standard kernel, and standard kernel plus ASIR 30% techniques. *Int J Radiol*. 2015;2(2):60-65. [Crossref]
22. Chatzaraki V, Kubik-Huch RA, Thali M, Niemann T. Quantifying image quality in chest computed tomography angiography: evaluation of different contrast-to-noise ratio measurement methods. Acta Radiol. 2022;63(10):1353-1362. [Crossref]
23. Tang H, Yu N, Jia Y, et al. Assessment of noise reduction potential and image quality improvement of a new generation adaptive statistical iterative reconstruction (ASIR-V) in chest CT. *Br J Radiol*. 2018;91(1081):20170521. [Crossref]
24. Guziński M, Waszczuk Ł, Sąsiadek MJ. Head CT: image quality improvement of posterior fossa and radiation dose reduction with ASiR - comparative studies of CT head examinations. *Eur Radiol*. 2016;26(10):3691-3696. [Crossref]
25. Smith-Bindman R, Chu PW, Azman Firdaus H, et al. Projected lifetime cancer risks from current computed tomography imaging. JAMA Intern Med. 2025;185(6):710–719. [Crossref]